Characterization of the discoidal complexes formed between apoA-I-CNBr fragments and phosphatidylcholine

Berlinda Vanloo,* John Morrison,† Noel Fidge,† Genevieve Lorent, Laurence Lins,** Robert Brasseur,** Jean-Marie Ruysschaert,** Johan Baert, †† and Maryvonne Rosseneu***

Department of Clinical Chemistry,* A.Z. St-Jan, B-8000 Brugge, Belgium; Baker Medical Research Institute,† Melbourne, Australia; Free University of Brussels,** Brussels, Belgium; and Interdisciplinary Research Centre, University of Leuven Campus Kortrijk,†† Kortrijk, Belgium

Abstract The structure, composition, and physico-chemical properties of lipid-protein complexes generated between dimyristoylphosphatidylcholine (DPMC) and the CNBr fragments of human apoA-I were studied. The fragments were separated by high performance liquid chromatography and purified on a reversed-phase column. The complexes with DMPC were isolated on a Superose column; their dimensions were obtained by gradient gel electrophoresis and by electron microscopy. The secondary structure of the protein in the complexes was studied both by circular dichroism and by attenuated total reflection infrared spectroscopy. The fragments 1 and 4 of apoA-I, containing, respectively, two and three amphipathic helices, recombined with the phospholipid to generate discoidal particles with sizes similar to that of apoA-I- and apoA-II-DMPC complexes. The infrared measurements indicated that in all complexes the apolipoprotein helical segments were oriented parallel to the phospholipid acyl chains and that the protein was located around the edges of the discs. Computer modelling of the complexes based on energy minimization techniques proposed a model for these particles in agreement with the dimensions measured experimentally. In conclusion, we propose that apoA-I and its longest CNBr fragments are able to generate discoidal particles with DMPC, with apolipoprotein helical segments oriented parallel to the acyl chains of the phospholipids. **—Vanloo, B., J. Morrison, N. Fidge, G. Lorent, L. Lins, R. Brasseur, J-M. Ruysschaert, J. Baert, and M. Rosseneu.** Characterization of the discoidal complexes formed between apoA-I-CNBr fragments and phosphatidylcholine. *J. Lipid Res.* 1991. **32:** 1253–1264.

Supplementary key words apolipoprotein • phospholipid • lipid-protein interaction • helical content • computer modelling

The reassembly of plasma apolipoproteins with lipids has been extensively studied (1–3). At defined phospholipid/protein ratios, discoidal particles consisting of lecithin, cholesterol, and apolipoprotein A-I can be generated (3). Such particles are good substrates for the enzyme lecithin:cholesterol acyltransferase (LCAT) (3).

Several amphipathic helical segments were identified within the apoA-I sequence and proposed to be involved in the lipid-apolipoprotein binding (4, 5). It is, however, not yet clear whether all segments interact directly with the phospholipids and which part of the molecule is responsible for the LCAT activation. Experiments with synthetic peptides were designed for this purpose: Sparrow and Gotto (6) synthesized five peptides representing sequences located between residues 142 and 185 of apoA-I and compared their LCAT activation properties. The longest peptide retained only 24% activity as compared to apoA-I, when micellar substrates were used for the LCAT reaction, while the activity of the other peptides decreased with their length. According to Fukushima et al. (7), the 121–164 residue segment of apoA-I is 30% as active as native apoA-I. Synthetic peptide analogues (8) of amphipathic helices were also able to active LCAT, although to a lesser extent than apoA-I. Recently, Anantharamaiah et al. (9) synthesized 22-residue and 44-residue peptides representing the consensus sequence for the helical repeats of apoA-I and compared their activity using both micellar and discoidal egg-phosphatidylcholine-cholesterol-peptide substrates. According to these authors (9), the major LCAT-activating domain of apoA-I consists of 22mer tandem repeats each containing Glu at the 13th residue and located between residues 66 and 121 of apoA-I.

As apoA-I contains three Met residues at positions 86, 112, and 148, the CNBr fragments seem appropriate to investigate the LCAT-activating properties of four different domains in apoA-I. Experiments carried out previously (10) suggested that the longest fragments activate LCAT

Abbreviations: DMPC, dimyristoylphosphatidylcholine; LCAT, lecithin:cholesterol acyltransferase; FPLC, fast protein liquid chromatography; ATR, attenuated total reflection; LDL, low density lipoproteins; HPLC, high performance liquid chromatography; DPH, diphenyl hexatriene; CD, circular dichroism.

to about 20–25% the extent of apoA-I, while the shorter fragments had no activity.

Since those preliminary experiments were carried out, more is known now about substrate specificity and optimal conditions for the LCAT activation (11). It is now clear that the physico-chemical properties of the apolipoprotein-lipid complexes largely determine the extent of activation (12). We therefore investigated the lipid-binding properties of the CNBr fragments of apoA-I as determinants for their LCAT activation properties. A comparison of the behavior of the four fragments should provide information about the regions of apoA-I involved in lipid binding and in LCAT activation and also about the structural features required for the formation of discoidal complexes.

MATERIALS AND METHODS

Isolation of apoA-I fragments

The apoA-I fragments were prepared by digestion with CNBr in 70% trifluoroacetic acid (TFA) for 24 h. CNBr digestion yields four fragments with respective lengths of 1–86, 87–112, 113–148, and 149–243 residues and with corresponding molecular weights of 9880, 3190, 4250, and 10700 Da. Fragments 1 and 2 contain, respectively, three Trp at positions 8, 50, 72, and one at residue 108. After drying under vacuum, the material was dissolved in the 50 mM Na citrate, 6 M urea buffer (pH 3.8) and applied to a Sephadex G50 column (2.5 × 200 cm), equilibrated with the same buffer. The fractions were further purified by reversed-phase HPLC on a RP300 column (20 μm particle size, 30 nm pore size, 10 × 100 mm i.d., Brownlee Laboratories, Santa Clara, CA), equilibrated with 0.1% TFA (13). The peptides were eluted with a linear gradient from 0 to 60% acetonitrile at a flow rate of 2 ml/min and continuously monitored at 280 nm using a Beckman Model 163 variable wavelength detector. Purity of the fragments was checked by SDS polyacrylamide gel electrophoresis and the amino acid composition was verified by amino acid analysis (13).

Complex isolation and characterization

Complexes were obtained by incubation of apoA-I, apoA-II, and of the apoA-I fragments with dimyristoylphosphatidylcholine (DMPC, Sigma) vesicles at DMPC/peptide (w/w) ratios of 5/1, 2/1, 1/1 at 25°C for 16 h. They were isolated by gel chromatography on a Superose 6HR column in 0.01 M Tris-HCl buffer, pH 7.6, in an FPLC system (Waters). For detection of the complexes the absorbance at 280 nm was monitored continuously and the Trp or Tyr emission of the fractions was measured on an Aminco SPF500 spectrofluorimeter. For further measurement of the composition and size of the complexes, the two fractions with maximal UV absorption in the elution peak of the complexes in the chromatographic runs were collected.

The composition of the complexes was determined by quantitation of the phospholipids using an enzymatic assay (Biomérieux, France). Peptide quantitation was carried out by determination of the phenylalanine by HPLC on a C18 reversed-phase column, after peptide hydrolysis (5). The size of the complexes was estimated by gradient gel electrophoresis in a 4–30% polyacrylamide gradient. The gels were scanned using a laser densitometer (Pharmacia, Uppsala, Sweden), and the Stokes radii were estimated from protein standards (Pharmacia).

Fluorescence measurements

The measurements of the Trp fluorescence emission in apoA-I and in fragments 1 and 2 and that of Tyr in apoA-II and in fragments 3 and 4, were used to monitor complex formation. The fluorescence measurements were performed on an Aminco SPF-500 spectrofluorimeter equipped with a special adapter (Aminco-J4-9501) for the fluorescence polarization measurements. The fluorescence polarization of the lipid-peptide complexes, labeled with diphenyl hexatriene (DPH) (molar ratio of lipid-DPH 500:1) was measured as a function of the temperature to detect changes in the fluidity of the phospholipid acyl chains due to lipid-peptide association. The excitation wavelength was set at 365 nm and emission was detected at 427 nm. Temperature scans between 15 and 40°C were performed using a circulating water bath (Julabo) at a rate of 0.6°C/min.

Fluorescence quenching of tryptophan residues was followed to monitor the accessibility of these residues in the intact protein, in fragment 1, and in the respective complexes. For this purpose, the fluorescence emission intensity of the Trp was followed at increasing concentrations of acyrlamide between 0 and 0.2 M. Results were analyzed according to the Stern-Volmer equation by plotting the ratio of the fluorescence intensity after and before quenching F/Fo, as a function of the inverse acrylamide concentration, and the Stern-Volmer constant was calculated from the slope of the regression line.

Electron microscopy of the lipid/peptide complexes

Phospholipid-peptide complexes, at a protein concentration of 150 μg/ml, were negatively stained with a 20 g/l solution of potassium phosphotungstate (pH 7.4). Seven μl of the samples was applied to Formvar carbon-coated grids and examined in a Zeiss EM 10C transmission electron microscope operating at 60 kV. Particle size was determined by measuring 120 discrete particles for each sample. The mean diameter and the size distribution of the complexes were calculated.

Cross-linking studies

To calculate the number of moles of protein per complex, cross-linking was performed with dithio-bis-succinimidyl propionate (DSP, Pierce Chemicals) followed by electrophoresis on SDS-gradient gels, according to the procedure of Swaney (14). Cross-linked apoA-I, comprising monomer, dimer, trimer, and oligomeric forms characteristic of this apolipoprotein, was used to calibrate the gels for molecular weight determinations (14). The cross-linking experiments were performed with the lipid/peptide complexes at a 2:1 (w/w) ratio.

Infrared spectroscopy measurements

Attenuated Total Reflection (ATR) infrared spectroscopy was used for the determination of the relative orientation of the apolipoprotein α-helical segments and of the phospholipid acyl chains as previously described for apoA-I- and apoA-II-phospholipid complexes and for LDL (5, 15). For these measurements, a 70-μl solution of 20 μg isolated complex in 0.005 M Tris-HCl buffer (pH 8.4) was spread on an ATR Germanium crystal plate. Deuteration of the sample was performed by flushing N_2, saturated with D_2O, in a sealed universal Perkin-Elmer sample holder, at room temperature for 3 h, in order to avoid overlapping of the absorption bands for random and α-helical structures.

Spectra were recorded on a Perkin-Elmer 1720 × infrared spectrophotometer, using polarized incident light with a perpendicular (90°) and parallel (0°) orientation. A dichroic spectrum was obtained by subtracting the spectrum recorded with polarized light at 0° from that at 90°. A positive deviation on the dichroic spectrum indicates a dipole preferentially oriented close to a normal to the plane, while a larger absorbance at 0° is indicative of a dipole oriented close to the Ge crystal plane. The angle between a normal to the Ge crystal and the dipole is obtained from the calculation of the dichroic ratio R_{atr} = A(90°)/A(0°), representing the ratio of the absorbances on the spectra recorded with polarized light at 90° and 0°. For each experiment up to 15 scans were stored and averaged.

Circular dichroism measurements

Circular dichroism spectra of the peptides and their complexes with lipids were measured on a Jasco 600 spectropolarimeter at 23°C (5). Measurements were carried out at a protein concentration of 0.1 mg/ml in a 0.01 M sodium phosphate buffer, pH 7.4. Nine spectra were collected and averaged for each sample. The secondary structure was estimated according to the generalized inverse method of Compton and Johnson (16).

Denaturation experiments

The stability of the DMPC-apoA-I and CNBr fragment 1-DMPC complexes was compared by following the maximal emission wavelength of the Trp residues after exposure to increasing quantities of GdmCl. For these experiments, aliquots of an 8 M GdmCl solution were added to the complex in a Tris-HCl buffer, pH 7.5.

Computer modelling

The computer-aided three-dimensional modelling was carried out as previously described (5). Briefly, the amphipathic helical segments were oriented and minimized at the lipid/water interface taking into account the hydrophobic and hydrophilic transfer energies. For each helix the hydrophobic and hydrophilic transfer energies were calculated by moving a 6 Å window along the axis. The computation of a spline function yielded the hydrophobic and hydrophilic transfer energy profile along the long axis of the helical segment.

The helices were further oriented as suggested from the infrared data and assembled together with the phospholipids, using a procedure modified from the method used to surround a drug with phospholipids (17). After defining the initial position of the helices, their coordinates were modified by stepwise translation of 0.5 Å in each direction and by rotation of 2.5° along the different axis. In order to further minimize the interaction energy between helices, the sum of the van der Waals, electrostatic, and hydrophobic interactions was calculated at each position. This gradient procedure was carried out until the lowest energy state of the entire complex was reached. The dimensions of the discoidal particle were measured from the constructed model.

Computations were performed on an Olivetti M380-XP5 microcomputer using an Intel 80387 arithmetic coprocessor with the PC-TAMMO (theoretical analysis of molecular membrane organization) procedures. Graphs were drawn with the PC-MGM + (Molecular Graphics Manipulation) program (5).

RESULTS

Reassembly of apoA-I fragments with phospholipids

The formation of small discoidal particles between DMPC vesicles and the apoA-I fragments was monitored by measuring the turbidity decrease at 325 nm as a function of temperature. **Fig. 1** shows that a scan through the transition temperature of DMPC decreases the turbidity of the mixtures prepared with the apoA-I and with fragments 1 and 4. The effect observed with fragments 2 and 3 was similar to the behavior of pure DMPC, suggesting no significant change of the particle size.

Complex formation was further monitored by measuring the Trp fluorescence emission spectrum in fragments 1 and 2 and that of Tyr in fragments 3 and 4. The maximal emission wavelength for fragments 1 and 2 lies,

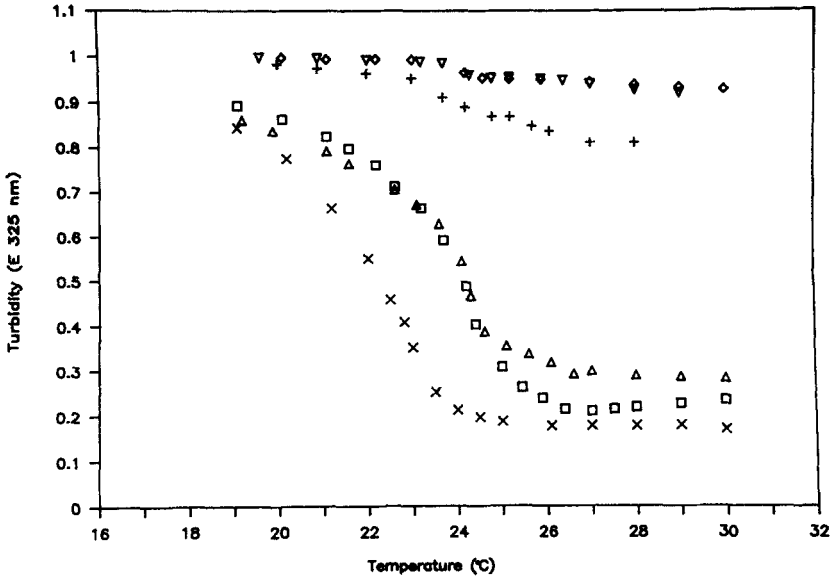

Fig. 1. Turbidity-decrease of mixtures of apoA-I and apoA-I-CNBr fragments with DMPC as a function of temperature, monitored by absorption measurements at 325 nm; (▽), DMPC; (×), apoA-I; (□), fragment 1; (+), fragment 2; (◇), fragment 3; (△), fragment 4.

respectively, at 346 and 355 nm, indicative of an exposed conformation of the Trp to the solvent. A blue shift to 334 nm was observed for fragment 1 upon phospholipid binding due to the more hydrophobic environment of the Trp in the complex. For fragment 2 no shift was observed. For comparison, in apoA-I the Trp emission wavelength was shifted from 333 to 329 nm only, suggesting that these residues are in a more hydrophobic environment in the intact protein than in the fragments. The emission maximum of Tyr in fragments 3 and 4 remained unchanged at 309 nm in the complex.

Measuring the degree of fluorescence polarization, after labeling with DPH was also used to follow complex formation. A decrease of the fluorescence polarization, indicative of a decreased mobility of the phospholipid acyl chains, was observed between 15° and 35°C corresponding to the crystalline to liquid crystalline transition of the DMPC acyl chains (**Fig. 2**). In the presence of apoA-I and of the CNBr fragments 1 and 4, the cooperativity of the transition decreased while the transition temperature increased. These data suggest that the peptide-lipid interactions decrease the mobility of the DMPC acyl chains. This was not observed with fragments 2 and 3 (Fig. 2), which in contrast to fragments 1 and 4 had a fluidizing effect on DMPC below the transition temperature. This observation suggests that weak interactions occurred that decreased the crystalline structure of DMPC, but were not sufficient to generate small discoidal complexes.

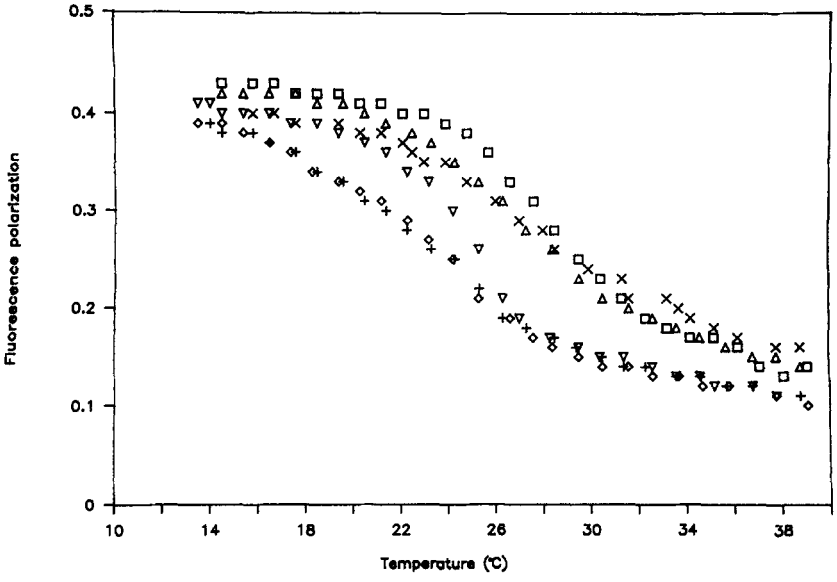

Fig. 2. Fluorescence polarization-decrease of apoA-I-CNBr fragments-DMPC mixtures as a function of temperature, after labeling with diphenylhexatriene; (▽), DMPC; (×), apoA-I; (□), fragment 1; (+), fragment 2; (◇), fragment 3; (△), fragment 4.

Separation and characterization of the DMPC-peptide complexes

The lipid-protein complexes between apoA-I, apoA-II, the apoA-I-CNBr fragments, 1, 2, 3, and 4 and DMPC at a 5/1 lipid/protein (w/w) ratio were fractionated on a Superose 6HR column (**Fig. 3**). Similar complexes, generated at lipid/protein (w/w) ratios of 1/1 and 2/1 were fractionated on the same column (**Fig. 4**). The presence of apoA-I and of the peptide fragments 1 and 2 could be detected by measurement of the Trp emission at 330 nm (Figs. 3A, 4A, 4C). The positions of fragments 3 and 4 of apoA-I, that of apoA-II, and of the corresponding complexes were monitored by measurement of the Tyr emission at 305 nm, (Figs. 3B, 4B, 4D). The complexes, generated through reassembly of apoA-I-CNBr fragments 1 and 4 with DMPC, eluted at a volume comparable to that of the apoA-I-DMPC complex (Figs. 3A, 3B). A small amount of fragment 1, eluting as free peptide at 20–23 ml, was also detected. Peptide fragments 2 and 3 recombined poorly with DMPC; only a small amount of complex with a size larger than the apoA-I/DMPC complex was detected, while most of the material eluted as free peptide (Figs. 3A, 3B). The size of the complexes generated with apoA-I and with fragments 1 and 4 (Figs. 4C, 4D) increased at increasing lipid/protein ratio. At all ratios tested, the complex yield was significantly higher with fragment 4 compared to fragment 1.

The complex composition, corresponding to the maxima of the elution peak of the complex in chromatographic elution patterns (Fig. 4), was obtained from phospholipid and peptide assays. The complex composition is summarized in **Table 1**, together with the number of peptides per complex obtained by cross-linking experiments and with the diameters of the complexes obtained by gradient gel electrophoresis and by electron microscopy (Figs. 5 and 6). Before fractionation by gel chromatography, the initial lipid-protein mixture was more heterogeneous. In addition to a major band, corresponding to the top fraction of the eluate, minor bands of complexes with larger diameters (around 110 Å) were also observed. Incubations carried out at various lipid/protein ratios showed that the lipid content of the isolated complexes increased with that of the original mixture (Table 1). For apoA-II at an initial lipid/protein ratio of 5/1, two complexes could be resolved with different size and composition, one similar to that generated with apoA-I under the same conditions, and the other larger and containing more lipid (Fig. 4B).

Estimation by gradient gel electrophoresis of the diameters of the various complexes generated with apoA-I, apoA-II and with the apoA-I-CNBr fragments showed that the diameter increased with increasing lipid/protein ratio in the complexes (Table 1). For every incubation mixture of apoA-I with DMPC, two complexes were

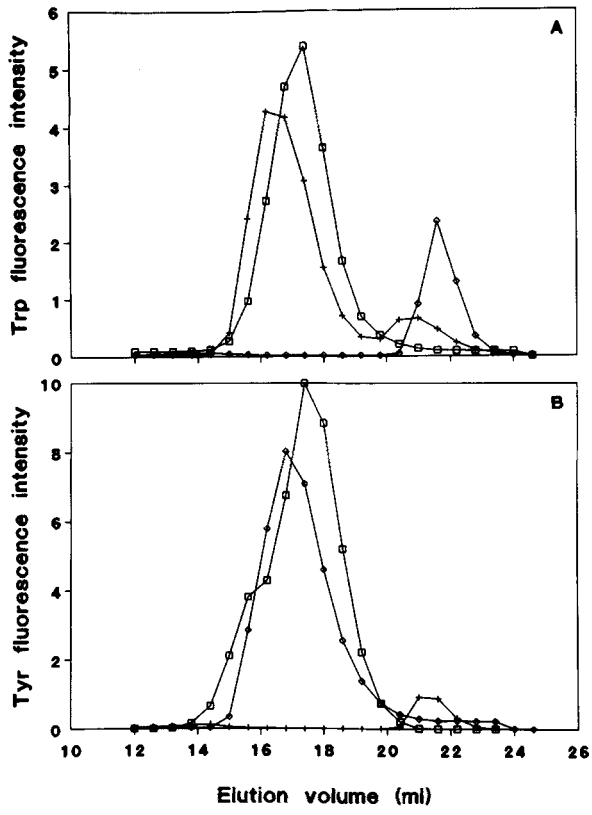

Fig. 3. Elution profiles of apoA-I CNBr fragments-DMPC complexes at a 5/1 (w/w) lipid/protein ratio, separated on a Pharmacia Superose 6HR column (30 × 1.0 cm, 0.01 M Tris-HCl buffer, pH 7.6). The fluorescence emission of Trp (A) and of Tyr (B) was used to monitor the peptide elution. A: (□), apoA-I; (+), fragment 1; (◇), fragment 2. B: (□), apoA-II; (+), fragment 3: (◇), fragment 4.

resolved in the top fraction of the gel filtration run (**Fig. 5**, lane 1), with a difference of 4 Å in diameter (Table 1). A more heterogeneous distribution was observed in the corresponding chromatographic fractions for the CNBr fragments 1 and 4 (Fig. 5, lanes 2, 3). This might be due to lesser constraints in the mode of assembly of the apoA-I fragments with lipids, as these consisted of, respectively, two and three helices, compared to seven helices for apoA-I. At an identical initial lipid/protein ratio, the diameters of the complexes generated either with apoA-I or with the CNBr fragments 1 and 4 were comparable.

The electron microscopic analysis of the same chromatographic fractions of the complexes showed the typical pattern of rouleaux, characteristic of stacked discs (**Fig. 6**). The diameter and distribution of the particles were determined by measurement of the electron micrographs. As observed for the gradient gel profiles, the size of the complexes obtained by electron microscopy increased at increasing lipid/protein ratio in the complex (Fig. 6). The size of the complexes assessed from electron microscopy was about 20–30 Å larger than that obtained from gradient gel electrophoresis. This might be due to flattening

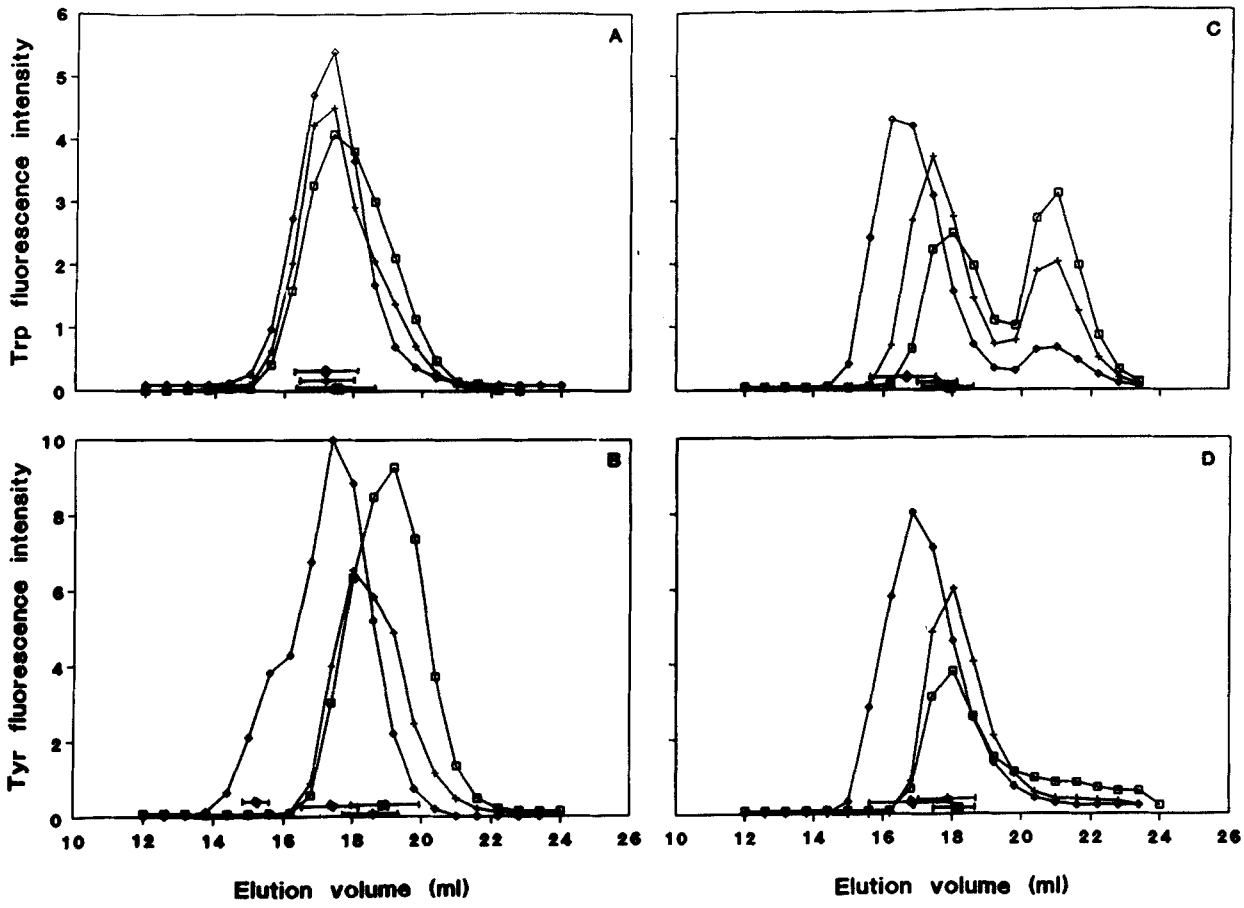

Fig. 4. Elution profiles of apoA-I-CNBr fragments-DMPC and apoA-II-DMPC complexes at a 5/1 (◇), 2/1 (+) and 1/1 (□), (w/w) lipid/protein ratio, separated on a Pharmacia Superose 6HR column (30 × 1.0 cm, 0.01 M Tris-HCl buffer, pH 7.6). The fluorescence emission of Trp (A, C) and of Tyr (B, D) was used to monitor the peptide elution. The bars under the elution peaks indicate the fractions that were pooled for the subsequent analyses. A: apo-A-I; B: apoA-II; C: fragment 1; D: fragment 4.

of the complexes during sample preparation and to electron irradiation (18).

Stability of the complexes

Denaturation experiments monitoring the Trp emission could only be performed on apoA-I and on fragment 1, as fragment 2 associated poorly with lipids while fragments 3 and 4 contained only Tyr residues. These experiments, performed by titration with increasing GdmCl concentrations, showed that the exposure of the Trp residues in apoA-I and in the CNBr fragment 1 increased with the GdmCl concentration (**Fig. 7**). As shown on Fig. 7, the native structure of fragment 1 is less ordered than that of apoA-I, as the Trp maximal wavelength lies at 346 compared to 334 nm in apoA-I. The mid-point of the transition is also shifted towards lower GdmCl concentrations and lies around 0.3 M for fragment 1 compared to 0.8–1 M for apoA-I. The association with lipids stabilizes the protein structure and protects it against denaturation, as the Trp emission shifts towards lower wavelengths in the complexes and the mid-point of the denaturation increases up to 2 and 4 M GdmCl for the fragment 1 and the intact apoA-I, respectively.

The fluorescence quenching experiments performed with acrylamide support the above observations and also indicate that the Trp residues are more accessible in fragment 1 than in intact apoA-I, as the Stern-Volmer Kav constants are 10.5 and 3.1 respectively (data not shown). Association with DMPC decreases the Trp exposure to the aqueous phase with a decrease of the Kav constant to 2.8 and 1.7 for fragment 1- and apoA-I-DMPC complexes. Denaturation with GdmCl unfolds the protein structure and exposes the Trp to the solvent with a concomitant increase of the Kav value to, respectively, 11.9 and 5.3 for apoA-I-CNBr fragment 1 and for the corresponding complex with DMPC.

TABLE 1. Composition and size of the complexes generated between DMPC, apoA-I, apoA-I-CNBr fragments (CF1 and CF4), and apoA-II

Mixture	Incubation Mix DMPC/Peptide	Complex DMPC/Peptide	GGE Stokes Diameter[a]	EM Diameter[b]	Peptide/ Complex[c]
	w/w	*mol/mol*	*Å*	*Å*	*mol/mol*
DMPC/A-I	1/1	99	104, 108 (± 2)	120 ± 20	
DMPC/A-I	2/1	120	104, 108 (± 2)	128 ± 22	2
DMPC/A-I	5/1	116	106, 108 (± 2)	151 ± 19	
DMPC/CF1	1/1	22	100, 104 (± 2)	124 ± 19	
DMPC/CF1	2/1	37	108, 110 (± 2)	130 ± 19	6
DMPC/CF1	5/1	50	138, 142 (± 2)	173 ± 22	
DMPC/CF4	1/1	28	102, 104 (± 2)	115 ± 15	
DMPC/CF4	2/1	36	106, 108 (± 2)	126 ± 19	5
DMPC/CF4	5/1	51	140, 144 (± 2)	167 ± 24	
DMPC/A-II	1/1	45	94, 96 (± 2)		
DMPC/A-II	2/1	69	94, 96 (± 2)		
DMPC/A-II	5/1	113	108, 110 (± 2)		
		131	140, 144 (± 2)		

[a]Obtained from gradient gel electrophoresis on nondenaturing gels by reference to standard proteins. The reproducibility of the diameter measurements is within ± 2 Å.

[b]Measured from electron micrographs of negatively stained samples. Means ± SD of the diameters are given for n = 120.

[c]From electrophoresis on SDS-gradient gels of the complexes crosslinked with dithio-bis-succinimidyl propionate (DSP) by reference to lipid-free apoA-I crosslinked in solution.

Determination of the helical content and of the orientation of the helices in the complexes

The secondary structure of the complexes was obtained both from the CD and IR measurements (**Table 2**). The secondary structure of the pure peptides was also measured by CD, and as previously observed for apoA-I (5), the binding to phospholipids increased the α-helical content of fragments 1 and 4 by 8–12% without affecting the β-sheet content (data not shown). Compared to the IR measurements, the CD data tend to underestimate the α-helical contribution of the peptide/lipid complexes and to overestimate the percentage of random structure and β-turns, as observed for the apoA-I-DMPC complex and for LDL (15). This might be due to differences in the method of analysis and the curve-fitting procedures used in the two techniques. The calculation of the helical content from the CD data relies on the curve fitting procedure of Compton and Johnson (16), which requires molar ellipticity data down to 184 nm. Previous estimations of the helical content, based upon molar ellipiticity values measured at 208 nm, probably overestimated the helical content of the apolipoproteins and of their complexes with lipids (1).

In order to determine the orientation of the α-helices with respect to the DMPC bilayer, ATR infrared spectra of DMPC and of the isolated complexes formed between

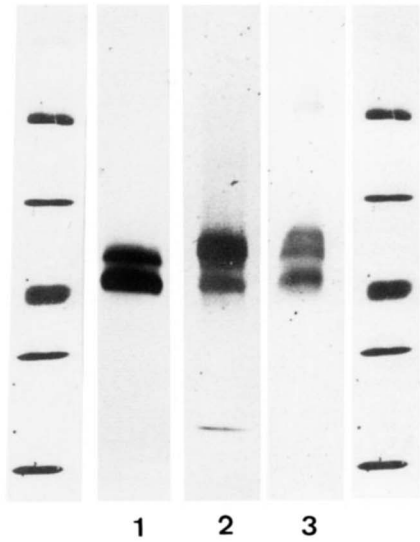

Fig. 5. Gradient gel electrophoresis separation of the complexes generated at an initial lipid/protein ratio of 2/1 (w/w) between DMPC, apoA-I, and apoA-I-CNBr fragments. The complexes correspond to the top fractions isolated by gel chromatography on the Superose 6HR column. The electrophoretic separation was carried out in a 4–30% polyacrylamide gradient and diameters were determined by comparison with known standards after scanning of the gels. Lane 1: apoA-I-DMPC, lane 2: apoA-I-CNBR fragment 4-DMPC; lane 3: apoA-I-CNBR fragment 1-DMPC complex. Standards, in order of decreasing diameter, are: thyroglobulin, ferritine, catalase, lactate dehydrogenase, bovine serum albumin.

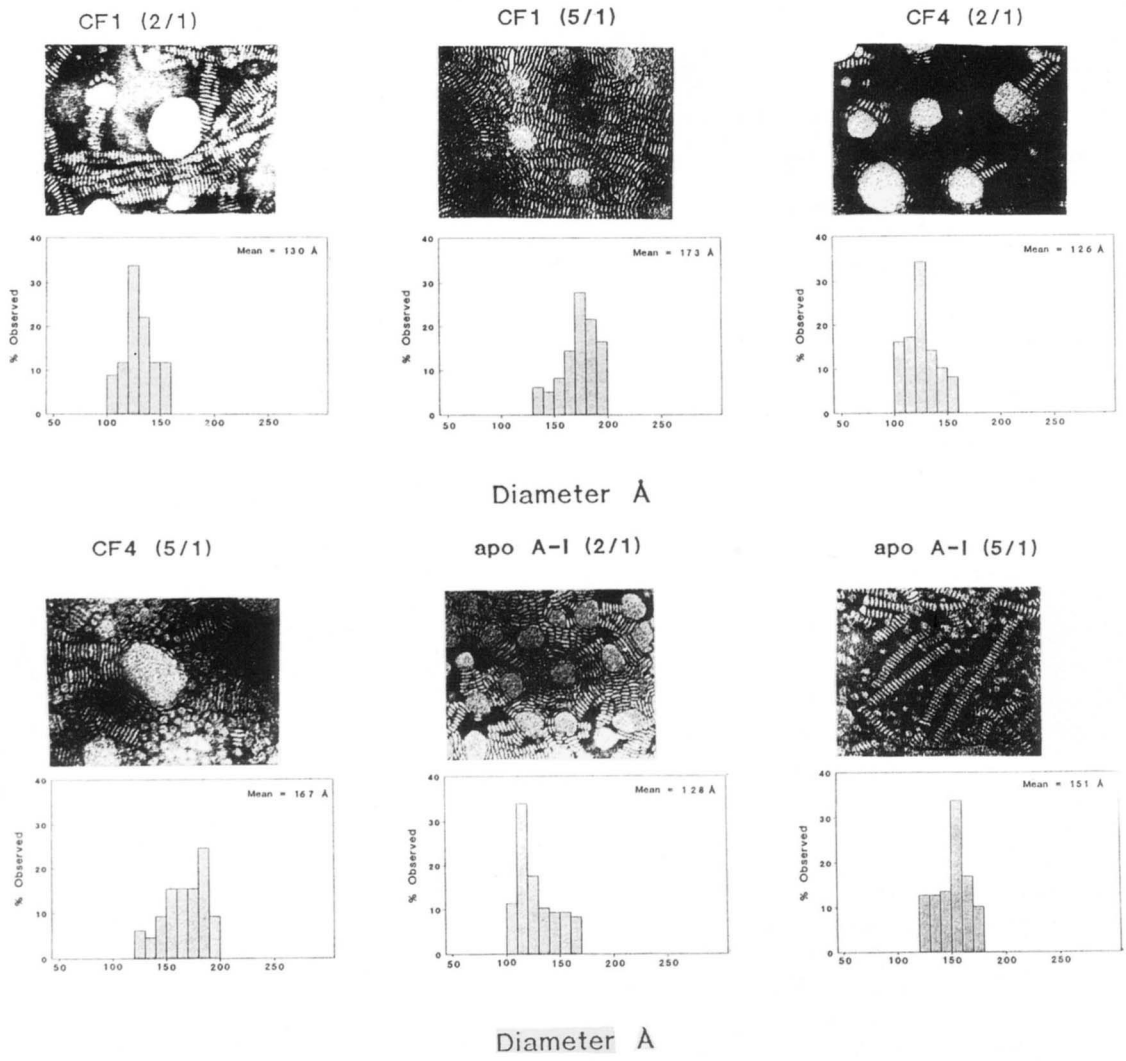

Fig. 6. Electron micrographs of negatively stained apoA-I-CNBr fragments-DMPC complexes at various DMPC/peptide ratios (w/w). The bar marker represents 60 nm. The mean diameter and the distribution, for n = 120 particles, are given for each sample. 1) Fragment 1, 2/1; 2) fragment 1, 5/1; 3) fragment 4, 2/1; 4) fragment 4, 5/1; 5) apoA-I, 2/1; and 6) apoA-I, 5/1.

the apoA-I fragments and DMPC were recorded at two orthogonal linear polarizations of the incident light (**Fig. 8**). The dichroic spectrum, obtained by subtracting the spectrum recorded with polarized light at 0° from that at 90°, is plotted on the same figure. A positive deviation of the dichroic spectrum at 90° indicates a dipole oriented preferentially close to a normal to the plane of the membrane, whereas a larger absorbance at 0° is indicative of a dipole close to the membrane plane.

In the apoA-I-fragments-DMPC complexes, a dichroic ratio R_{atr} of 7.3 was calculated for the acyl chains, indicating that the hydrocarbon chains are tilted at an angle of 24° from the normal to the Ge surface. This value is close to that measured for the apoA-I-DMPC complex (5), and higher than that for pure DMPC. The two carbonyl groups of DMPC (1736 cm^{-1}) are partially resolved in the dichroic spectrum (Fig. 8). The band assigned to the α-helical structure in the amide I' region with a maximum at 1654 cm^{-1} shows a strong polarization at 90°, as indicated by a positive deviation from the base-line, in the dichroic spectrum (Fig. 8). The dichroic ratios of the α-helical component measured for apoA-I, apoA-II, and for the CNBr fragments 1 and 4 were 1.73, 1.84, 1.85, and 1.56, respectively. These figures correspond to angles of respectively 25, 22, 22, and 30° of the long axis of the α-helix with a normal to the Ge plane. From these data, we can therefore assume that the helices and the phospholipid acyl chains are oriented parallel to each other.

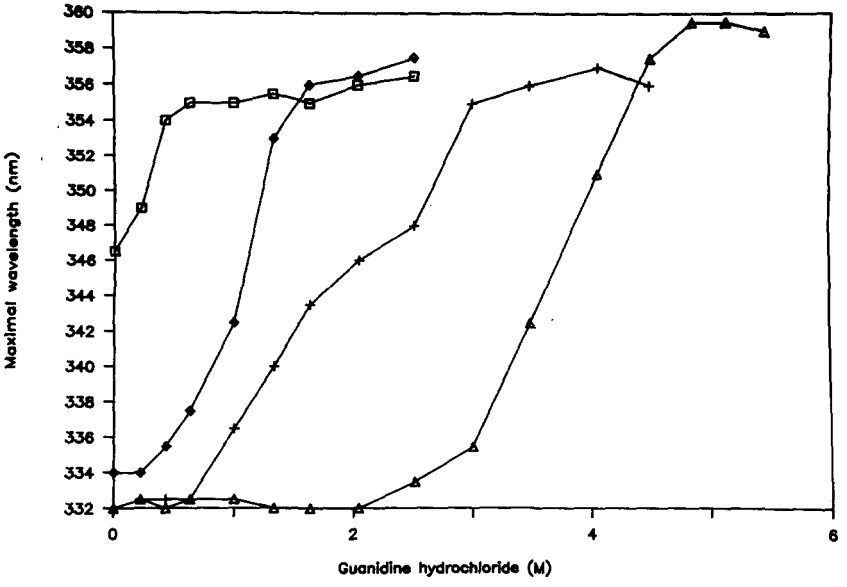

Fig. 7. Denaturation by GdmCl of apoA-I (◇), apoA-I-CNBr fragment 1 (□), apoA-I-DMPC (△), and apoA-I-CNBr fragment 1-DMPC complex (+) as monitored by the maximal Trp emission wavelength. The protein concentration was 50 μg/ml and aliquots of 8 M GdmCl were added to the complex in a Tris-HCl buffer, pH 7.5.

Overall structure of the apolipoprotein-phospholipid complexes

The number of helices in the apoA-I-lipid complex and in the peptide lipid complexes was estimated from the IR data. The results suggest that apoA-I contains seven 18-residue helical segments, while the CNBr fragments 1 and 4 contain, respectively, two and three 18-residue amphipathic helices. These helices correspond to the repeats previously identified in apoA-I as: residues 44–61 and 68–85 for fragment 1, and 167–184, 189–206, and 222–239 for fragment 4 (**Table 3**). The mean hydrophobicity index (Hi) and hydrophobic moment (μi), calculated using the consensus scale of Eisenberg, Weiss, and Terwilliger (19), were comparable for both fragments. The respective values for Hi and μi were 0.3 and 0.42 for fragment 1 and 0.45 and 0.3 for fragment 4. Based on the helical content of apoA-I, it seems that the 44–61 helix, which is the least stable when built by computer modelling, might not adopt a helical conformation in native apoA-I. In the CNBr fragment 1, however, its cooperativity with helix 66–85 probably increases the stability of its helical conformation in the lipid-apoprotein complex (5). Fragment 2 (residues 87–112) does not contain a full-length helix, but only 12 residues of the 101–118 helical repeat. This helix might not be sufficiently long and stable to bind lipids, as experiments with synthetic peptides previously suggested that 5–6 turns of an amphipathic helix are required for optimal lipid binding properties (6). In fragment 3 (residues 113–148), the 18-residue helix (123–140) is located between two β-turns which might prevent the parallel orientation of this helix with the phospholipid acyl chains, required to form stable discoidal particles.

The various helical segments listed in Table 3 were built by computer modelling and their diameters were determined. The diameters D1 and D2 were measured, respectively, parallel and perpendicular to a cross-section of the hydrophobic face, as shown on **Fig. 9**. Table 3 and Fig. 9 clearly demonstrate that the helices of apoA-I and apoA-II do not have a circular cross-section as the diameter D1 is larger than D2 by 2–5 Å. These helical segments thus have a slightly ellipsoidal shape with an axial ratio of 1.2.

When the peptides and the phospholipids were assembled in the complex, as previously carried out for apoA-I (5), a discoidal particle was obtained consisting of a phospholipid bilayer surrounded by 18-residue helical segments, as the β-turns at the ends of the helices are not included (5). These helices are oriented parallel to the phospholipid acyl chains as shown by IR measurements.

TABLE 2. Percentages of secondary structure of complexes determined by circular dichroism (CD) and infrared spectroscopy (IR) in complexes generated between DMPC and apoA-I, apoA-I CNBr fragments, and apoA-II

Secondary Structure	A-I + DMPC	A-II + DMPC	CF1 + DMPC	CF4 + DMPC
α-Helix				
CD	47.0	40.0	32.0	35.5
IR	48.8	58.5	44.4	53.5
β-Sheet				
CD	25.7	23.0	25.5	21.7
IR	25.1	22.5	35.4	25.7
β-Turns				
CD	14.7	20.4	15.0	15.2
IR	14.8	12.7	5.0	2.3
Random coil				
CD	12.6	18.1	27.5	27.6
IR	11.4	6.3	15.1	18.4

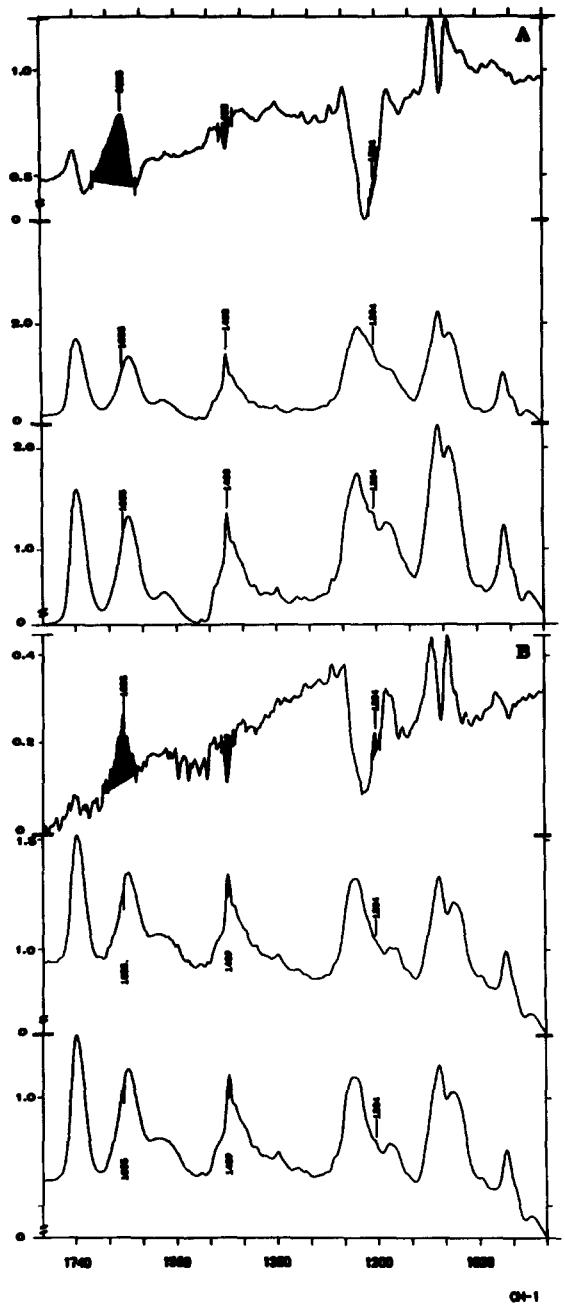

Fig. 8. Infrared spectra and difference spectra of DMPC complexes with apoA-I-CNBr fragment 1 (A) and fragment 4 (B), measured with polarized light at 0° (middle) and 90° (lower spectrum); upper spectrum corresponds to the 90–0° difference.

The mean distance between the centers of adjacent helices (Table 3) is 17.6 Å, compared to 16.3 Å for the largest diameter of the helices. This corresponds to an average distance between the outer residues of adjacent helices of 1.3 Å, indicating that the outer surface of the disc is covered for more than 90% by the protein segments.

The experimental values obtained by gradient gel electrophoresis for the outer diameter of the smallest discoidal complexes isolated at a 2:1 lipid/protein ratio, were used to estimate the number of helices that could be fitted around the edges of the discoidal particles. In these calculations, the mean diameter D2 of the helices was subtracted from the outer diameter of the disc. The calculated number of helices was compared to that estimated from the helical content of the complex obtained from the IR data (**Table 4**). The calculated number of helices was in all cases higher than that measured experimentally, suggesting that the helices are not as closely packed as theoretically possible. The value derived experimentally differs even more from that calculated assuming a mean diameter of 15 Å per helix (20), in agreement with the observation that the diameter of the apolipoprotein helical segments is larger tangentially to the edges of the discoidal complexes. Assuming an area of 50 $Å^2$/molecule of DMPC (5), the number of phospholipids per disc was further calculated from the experimental value obtained for the outer diameter of the complexes. Table 4 shows that there is a reasonable agreement between the calculated values and those derived from the experimental lipid and peptide compositions listed in Table 1.

TABLE 3. Values measured by computer modelling for the diameters D1 and D2 and the distance d between the centers of adjacent helices in a discoidal lipid/apolipoprotein complex

Helical Segment	D1	D2	d
		Å	
ApoA-I			
68–85	17.1	14.1	17.5
101–118	18.9	16.1	19.9
123–140	17.2	12.8	16.7
145–162	15.3	11.4	18.8
167–184	15.0	10.4	16.1
189–206	15.3	13.0	16.8
222–239	16.0	13.4	
< >	16.3	12.9	17.6
CF1			
44–61	16.4	13.1	17.8
68–85	17.1	14.1	
< >	16.8	13.6	17.8
CF4			
167–184	15.0	10.4	16.1
189–206	15.3	13.0	16.8
222–239	16.0	13.4	
< >	15.4	12.3	16.4
ApoA-II			
11–28	16.8	13.1	16.6
52–69	15.9	14.0	
< >	16.3	13.5	16.6

The diameter D1 is measured tangentially and D2 perpendicular to the edges of the disc.

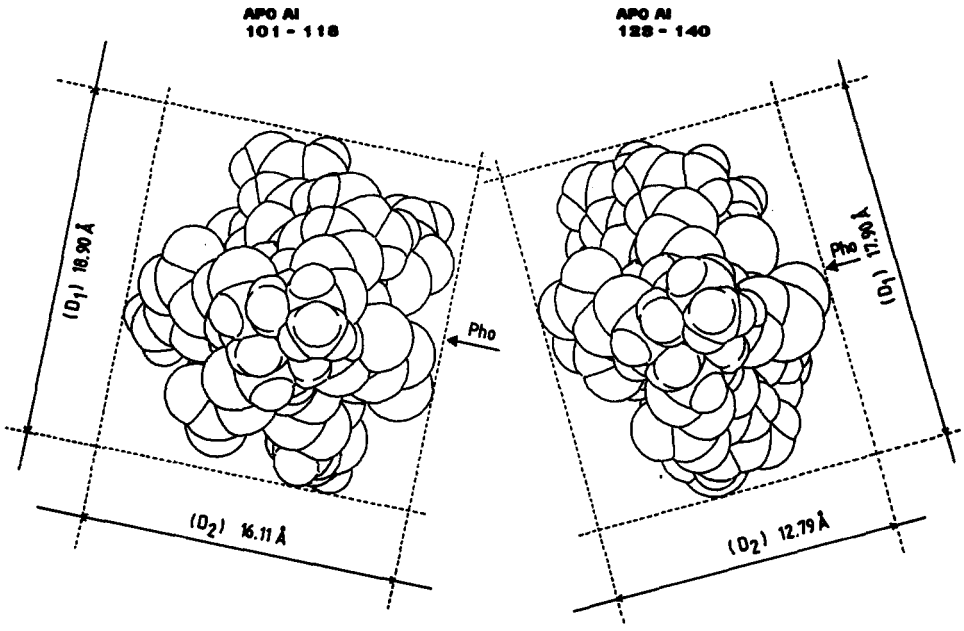

Fig. 9. Computer graphics representation of the top view of two helices (101–118, 123–140) of apoA-I, showing the ellipsoidal shape of the cross-section of the helices. The diameters D1 and D2 are measured parallel and perpendicular to the hydrophobic face of the helix. In both cases D1 is larger than D2 and the helices are oriented tangentially along the edges of the discoidal particles with D1 facing the aqueous phase.

CONCLUSIONS

The results obtained on the reassembly of apoA-I-CNBr fragments with DMPC suggest that the association of fragments 1 and 4 with lipids is similar to that of apoA-I. These fragments contain, respectively, two and three of the helical repeats identified in apoA-I and are therefore susceptible to recombination with DMPC to generate discoidal particles with a size comparable to that of the apoA-I-DMPC particles. Fragments 2 and 3 cannot generate the same type of complexes, probably because they do not contain one full-length helical segment able to span the thickness of the phospholipid bilayer. The presence of such helices, oriented parallel to the phospholipid acyl chains, seems therefore critical for the formation of these discoidal particles. ATR infrared measurements, carried out on apoA-I-, apoA-II-, and apoA-I-fragments-DMPC complexes have shown that these apolipoproteins are oriented around the edges of the discoidal complexes with the axis of the amphipathic segment parallel to the phospholipid acyl chains. One can therefore postulate that this is a general mechanism contributing to the formation of discoidal apoprotein-phospholipid particles. According to Chung et al. (21) and to recent observations by Anantharamaiah et al. (9), the lipid-binding and LCAT activation properties of a synthetic peptide consisting of two helical segments linked by a Pro residue are superior to those of the corresponding monomer. Yokohama et al. (22) had reached similar conclusions based on their work with synthetic peptide analogs of apoA-I. The cooperativity between apolipoprotein helical segments appears, therefore, as an important determinant of the stability of the lipid-apolipoprotein complexes.

From the structural data obtained on the apoA-I-phospholipid complexes (5) and from the present results one can therefore speculate that the formation of discoidal particles with helices around the edges of the disc is a prerequisite for the LCAT activation properties of these peptides. CNBr fragments 1 and 4 of apoA-I should therefore present such an activity, as suggested from literature data (6). However, as similar particles generated with

TABLE 4. Comparison of the experimental and calculated values for the protein and phospholipid (DMPC) composition of the isolated complexes generated at an initial lipid/protein ratio of 2/1, w/w

	Number of Helices		Moles of DMPC	
Complex	Experimental (IR)	Calculated	Experimental	Calculated
ApoA-I	12–14	16	240	265
CF1	12	16	222	288
CF4	15	18	180	228
ApoA-II	12	16	207	204

Experimental number of helices per discoidal complex was obtained from the infrared data. Phospholipid content was determined by chemical analysis. Number of DMPC was calculated assuming an area of 50 $Å^2$/phospholipid.

apoA-II do not serve as good substrates for LCAT, some additional features must be necessary to trigger the activation. Experiments are now in progress to test this hypothesis

G. Lorent is a recipient of a post-doctoral fellowship of the I.R.S.I.A. (Institut de Recherche Scientifique pour l'Industrie et l'Agriculture). We are grateful to M. J. Taveirne and H. Caster for excellent technical assistance.

Manuscript received 18 October 1990, in revised form 11 March 1991, and in re-revised form 2 May 1991.

REFERENCES

1. Pownall, H. J., J. B. Massey, J. T. Sparrow, and A. M. Gotto. 1987. Lipid-protein interactions and lipoprotein reassembly. *In* Plasma Lipoproteins. A. M. Gotto, editor. Elsevier Science, Amsterdam. 95–127.
2. Van Tornout, P., R. Vercaemst, M. J. Lievens, H. Caster, M. Rosseneu, and G. Assmann. 1980. Reassembly of human apoA-I and apoA-II proteins with unilamellar phosphatidylcholine-cholesterol liposomes. Association kinetics and characterization of the complexes. *Biochim. Biophys. Acta.* **601:** 509–523.
3. Jonas, A. 1987. Lecithin:cholesterol acyltransferase. *In* Plasma Lipoproteins. A. M. Gotto, editor. Elsevier Science, Amsterdam. 299–333.
4. De Loof, H., M. Rosseneu, R. Brasseur, and J. M. Ruysschaert. 1987. Functional differentiation of amphiphilic helices of the apolipoproteins by hydrophobic moment analysis. *Biochim. Biophys. Acta.* **911:** 45–52.
5. Brasseur, R., J. De Meutter, B. Vanloo, E. Goormaghtigh, J. M. Ruysschaert, and M. Rosseneu. 1990. Mode of assembly of amphipathic helical segments in model high density lipoproteins. *Biochim. Biophys. Acta.* **1043:** 245–252.
6. Sparrow, J. T., and A. M. Gotto. 1981. Apolipoprotein/lipid interaction: studies with synthetic polypeptides. *Crit. Rev. Biochem.* **13:** 87–107.
7. Fukushima, D., S. Yokoyama, D. J. Kroon, F. J. Kezdy, and E. T. Kaiser. 1980. Chain-length function correlation of amphiphilic peptides. Synthesis and surface properties of a tetracontapeptide segment of apolipoprotein A-I. *J. Biol. Chem.* **255:** 10651–10657.
8. Pownall, H. J., A. Hu, A. M. Gotto, J. J. Albers, and J. T. Sparrow. 1980. Activation of lecithin:cholesterol acyltransferase by synthetic model lipid-associating peptide. *Proc. Natl. Acad. Sci. USA.* **77:** 3154–3158.
9. Anantharamaiah, G. M., Y. V. Venkatachalapathi, C. G. Brouillette, and J. P. Segrest. 1990. Use of synthetic peptide analogues to localize lecithin:cholesterol acyltransferase activating domain in apolipoprotein A-I. *Arteriosclerosis.* **10:** 95–105.
10. Fielding, C. J., V. G. Shore, and P. E. Fielding. 1972. A protein cofactor of lecithin:cholesterol acyltransferase. *Biochim. Biophys. Res. Commun.* **46:** 1493–1499.
11. Jonas, A. 1986. Synthetic substrates of lecithin:cholesterol acyltransferase. *J. Lipid* **27:** 689–698.
12. Jauhianen, M., and P. J. Dolphin. 1986. Human plasma lecithin: cholesterol acyltransferase: an elucidation of the catalytic mechanism. *J. Biol. Chem.* **261:** 7032–7043.
13. Morrison, J., N. Fidge, and B. Grego. 1989. Studies on the formation, separation and characterisation of cyanogen bromide fragments of human A-I apolipoprotein. *Anal. Biochem.* **186:** 145–152.
14. Swaney, J. B. 1986. Use of cross-linking reagents to study lipoprotein structure. *Methods Enzymol.* **128:** 613–626.
15. Goormaghtigh, E., J. De Meutter, B. Vanloo, R. Brasseur, M. Rosseneu, and J. M. Ruysschaert. 1989. Evaluation of the secondary structure of apoB-100 in low density lipoprotein (LDL) by infrared spectroscopy. *Biochim. Biophys. Acta.* **1006:** 147–150.
16. Compton, L. A., and W. C. Johnson, Jr. 1986. Analysis of protein circular dichroism spectra for secondary structure using a simple matrix multiplication. *Anal. Biochem.* **155:** 155–167.
17. Brasseur, R., and J-M. Ruysschaert. 1986. Conformation and mode of organisation of amphiphilic membrane components: a conformational analysis. *Biochem. J.* **238:** 1–11.
18. Hayat, M. A., and S. E. Miller. 1990. Negative Staining. McGraw-Hill Publishing Co., New York.
19. Eisenberg, D., R. M. Weiss, and T. C. Terwilliger. 1984. The hydrophobic moment detects periodicity in the protein hydrophobicity. *Proc. Natl. Acad. Sci. USA.* **81:** 140–144.
20. Jonas, A., K. E. Kezdy, and J. W. Wald. 1989. Defined apolipoprotein A-I conformations in reconstituted high density lipoprotein discs. *J. Biol. Chem.* **264:** 4818–4824.
21. Chung, B. H., G. M. Anantharamaiah, C. G. Brouillette, T. Nishida, and J. P. Segrest. 1985. Studies of synthetic peptide analogues of the amphipathic helix: correlation of structure with function. *J. Biol. Chem.* **260:** 10256–10262.
22. Yokohama, S., D. Fukushima, J. P. Kupferberg, F. J. Kezdy, and E. T. Kaiser. 1980. The mechanism of action of LCAT by apolipoprotein A-I and an amphipathic peptide. *J. Biol. Chem.* **255:** 7333–7339.